HHS Public Access

Author manuscript

Clin Cancer Res. Author manuscript; available in PMC 2018 August 01.

Published in final edited form as:

Clin Cancer Res. 2017 August 01; 23(15): 4323–4334. doi:10.1158/1078-0432.CCR-16-2287.

HER2-overexpressing breast cancers amplify FGFR signaling upon acquisition of resistance to dual therapeutic blockade of HER2

Ariella B. Hanker[*,1,2], **Joan T. Garrett**[*,1,3], **Mónica Valeria Estrada**[2], **Preston D. Moore**[1], **Paula González Ericsson**[2], **James P. Koch**[1], **Emma Langley**[4], **Sharat Singh**[4], **Phillip S. Kim**[4], **Garrett M. Frampton**[5], **Eric Sanford**[5], **Philip Owens**[6], **Jennifer Becker**[1], **M. Reid Groseclose**[7], **Stephen Castellino**[7], **Heikki Joensuu**[8], **Jens Huober**[9], **Jan C. Brase**[10], **Samira Majjaj**[11], **Sylvain Brohée**[11], **David Venet**[11], **David Brown**[11], **José Baselga**[12], **Martine Piccart**[11], **Christos Sotiriou**[11], and **Carlos L. Arteaga**[1,2,6]

[1]Department of Medicine, Vanderbilt-Ingram Cancer Center, Vanderbilt University, Nashville, TN, USA [2]Breast Cancer Program, Vanderbilt-Ingram Cancer Center, Vanderbilt University, Nashville TN, USA [4]Prometheus Laboratories, San Diego, CA, USA [5]Foundation Medicine, Cambridge, MA, USA [6]Department of Cancer Biology, Vanderbilt University, Nashville, TN, USA [7]Department of Drug Metabolism and Pharmacokinetics, GlaxoSmithKline, Research Triangle Park, NC, USA [8]Department of Oncology, Helsinki University Central Hospital, Helsinki, Finland [9]Department of Gynecology, University of Ulm, Ulm, Germany [10]Novartis Pharmaceuticals, Basel, Switzerland [11]Institut Jules Bordet, Université Libre de Bruxelles, Brussels, Belgium [12]Department of Medicine, Memorial Sloan Kettering Cancer Center, New York, NY, USA

Abstract

Purpose—Dual blockade of HER2 with trastuzumab and lapatinib or pertuzumab has been shown to be superior to single-agent trastuzumab. However, a significant fraction of HER2-overexpressing (HER2+) breast cancers escape from these drug combinations. In this study, we sought to discover the mechanisms of acquired resistance to the combination of lapatinib + trastuzumab.

Corresponding author: Carlos L. Arteaga, Vanderbilt University Medical Center, 2220 Pierce Ave, 777 PRB, Nashville, TN 37232-6307. Phone: 615-936-0975; Fax: 615-343-7602; carlos.arteaga@vanderbilt.edu.

*These authors contributed equally.

[3]Current address: Division of Pharmaceutical Sciences, University of Cincinnati College of Pharmacy, Cincinnati, OH, USA

Conflict of interest statement: The authors have no competing financial interests.

Author contributions:

Conception and design: A. Hanker, J. Garrett, C. Sotiriou, C. Arteaga

Development of methodology: A. Hanker, J. Garrett, M. V. Estrada, P. Owens, E. Langley, S. Singh, P. Kim, G. Frampton, E. Sanford, M. R. Groseclose, S. Castellino, S. Brohée, D. Venet, D. Brown, C. Sotiriou, C. Arteaga

Acquisition of data: A. Hanker, J. Garrett, M. V. Estrada, P. Moore, P. Gonzalez Ericsson, J. Koch, E. Langley, G. Frampton, E. Sanford, P. Owens, J. Becker, M. R. Groseclose, S. Castellino, S. Majjaj, S. Brohée, D. Venet, D. Brown.

Analysis and interpretation of data: A. Hanker, J. Garrett, M. V. Estrada, P. Gonzalez Ericsson, E. Langley, S. Singh, P. Kim, G. Frampton, E. Sanford, P. Owens, M. R. Groseclose, S. Castellino, S. Brohée, D. Venet, D. Brown, C. Sotiriou, C. Arteaga

Acquisition of samples and/or collection of clinical data: H. Joensuu, J. Huober, J. Brase, J. Baselga, M. Piccart

Writing, review, and/or revision of manuscript: A. Hanker, J. Garrett, J. Brase, S. Brohée, D. Venet, D. Brown, C. Sotiriou, C. Arteaga

Study supervision: C. Sotiriou and C. Arteaga

Experimental Design—HER2+ BT474 xenografts were treated with lapatinib + trastuzumab long-term until resistance developed. Potential mechanisms of acquired resistance were evaluated in lapatinib + trastuzumab-resistant (LTR) tumors by targeted capture next-generation sequencing. *In vitro* experiments were performed to corroborate these findings and a novel drug combination was tested against LTR xenografts. Gene expression and copy number analyses were performed to corroborate our findings in clinical samples.

Results—LTR tumors exhibited an increase in *FGF3/4/19* copy number, together with an increase in FGFR phosphorylation, marked stromal changes in the tumor microenvironment, and reduced tumor uptake of lapatinib. Stimulation of BT474 cells with FGF4 promoted resistance to lapatinib + trastuzumab *in vitro*. Treatment with FGFR tyrosine kinase inhibitors reversed these changes and overcame resistance to lapatinib + trastuzumab. High expression of *FGFR1* correlated with a statistically shorter progression-free survival in patients with HER2+ early breast cancer treated with adjuvant trastuzumab. Finally, *FGFR1* and/or *FGF3* gene amplification correlated with a lower pathological complete response in patients with HER2+ early breast cancer treated with neoadjuvant anti-HER2 therapy.

Conclusions—Amplification of FGFR signaling promotes resistance to HER2 inhibition, which can be diminished by the combination of HER2 and FGFR inhibitors.

Keywords

HER2; FGFR; trastuzumab; drug resistance; breast cancer

Introduction

Approximately 20% of breast cancers harbor gene amplification of the receptor tyrosine kinase (RTK) HER2 (ERBB2) (1). HER2 is a member of the ERBB family of transmembrane RTKs. Upon ligand-induced dimerization, ERBB family receptors undergo conformational changes that trigger kinase activation and subsequent signal transduction through oncogenic pathways, such as phosphoinositide 3-kinase (PI3K)-Akt and RAS/RAF/MEK/ERK. Anti-HER2 therapies include trastuzumab (T), a humanized monoclonal antibody directed against the ectodomain of HER2; pertuzumab, an antibody that blocks dimerization of HER2 with other ERBB receptors; lapatinib (L), a reversible, ATP-competitive tyrosine kinase inhibitor (TKI) of HER2 and EGFR (2); and trastuzumab-DM1, a conjugate of trastuzumab linked to the chemotherapeutic maytansine. Recent clinical studies have shown that dual inhibition of HER2, such as the combination of L + T or T + pertuzumab, is more effective than trastuzumab (3–5). Despite these advances, resistance to dual HER2 blockade still occurs in patients with HER2+ breast cancer. The mechanisms of acquired resistance to dual HER2 inhibition remain to be fully explored.

Proposed mechanisms of resistance to HER2 inhibitors include the presence of truncated HER2, bypass signaling by other ERBB receptors or other RTKs, activation of compensatory survival pathways, defects in apoptosis and cell cycle control, and mutational activation of the PI3K pathway [reviewed in (2)]. We and others have previously shown that activating PIK3CA mutations can promote resistance to dual inhibition of HER2 (6–8).

In order to discover novel mechanisms of resistance to dual HER2 blockade, we generated HER2-amplified BT474 xenografts resistant to the combination of L + T. We found increased copy number of the *FGF3, FGF4*, and *FGF19* genes in L + T-resistant (LTR) tumors. The *FGF3/4/19* genes reside on chromosome 11q13, a region which also harbors *CCND1*, and is amplified in ~15% of breast cancers (The Cancer Genome Atlas (9); www.cbioportal.org (10)). The *FGF3/4/19* genes encode ligands for the Fibroblast Growth Factor Receptor (FGFR) family of RTKs (FGFR1-4). Aberrant FGFR signaling drives tumor cell proliferation, survival, angiogenesis, and activation of stromal fibroblasts, and has been associated with resistance to a number of targeted therapies (11). In addition, *FGFR1* is amplified in ~10% of breast cancers and is associated with poor patient prognosis (12,13). We show herein that 1) exogenous FGF promotes resistance to HER2 inhibition, 2) inhibition of treatment with FGFR tyrosine kinase inhibitors (TKIs) reversed or reduced resistance to L + T, and 3) somatic alterations in the FGFR pathway correlated with lack of benefit from anti-HER2 therapies in patients with early HER2+ breast cancer. These data suggest that FGFR pathway activation promotes resistance to L + T and support the combination of FGFR inhibitors with HER2-directed therapies in patients with HER2-overexpressing breast cancer.

Materials and Methods

Cell lines and inhibitors

BT474, HCC1954, and MDA-MB 361 cells were obtained from the American Type Culture Collection (ATCC) between 2006–2011 and maintained in ATCC-recommended media supplemented with 10% FBS (Gibco) and 1x antibiotic/antimycotic (Gibco). All cell lines were authenticated by ATCC using the short tandem repeat (STR) method in January 2017. Mycoplasma testing was conducted for each cell line before use. All experiments were performed less than 2 months after thawing early passage cells.

The following drugs were used: lapatinib (GW-572016, LC Laboratories), trastuzumab (Vanderbilt University Hospital Pharmacy), lucitanib (14) (provided by Clovis Oncology), and AZD4547 (15) (provided by AstraZeneca Pharmaceuticals).

Drug-resistant xenografts and mouse studies

A 21-day 17β estradiol pellet (Innovative Research of America) was inserted subcutaneously (s.c.) in the dorsum of 4- to 6-week-old female athymic mice (Harlan Sprague Dawley Inc.) one day before tumor cell injection. Approximately 5×10^6 BT474 cells were injected s.c. into the right flank of mice. Once tumors reached a size of ≥200 mm^3, mice were treated with 20 mg/kg trastuzumab diluted in sterile PBS by i.p. injection twice a week and 100 mg/kg lapatinib by orogastric gavage daily. Tumor diameters were serially measured with calipers and tumor volumes were calculated as: volume = $width^2 \times length/2$. Upon complete tumor regression with L + T, treatment was halted. Once tumors recurred (≥200 mm^3), treatment with lapatinib and trastuzumab was resumed. Recurrent tumors that progressed in the presence of L + T were serially transplanted into tumor-naïve nude mice. Once the transplanted tumors reached a volume ≥200 mm^3, mice were treated again with L + T.

Tumors growing in continuously treated mice were considered to be lapatinib/trastuzumab resistant (LTR).

For therapeutic studies, LTR tumors were transplanted into treatment-naïve mice following the same protocol. Once tumors reached a volume ≥200 mm^3, mice were randomized to any of these treatment arms: vehicle (0.5% hydroxypropylmethyl cellulose and 0.1% Tween-80); trastuzumab (20 mg/kg i.p. twice a week) and lapatinib (100 mg/kg by oral gavage daily); lucitanib (20 mg/kg by oral gavage daily); AZD4547 (12.5 mg/kg by oral gavage daily); or T +L plus each of the FGFR inhibitors. Tumors were harvested 24 h after the last dose of trastuzumab and 1 h after the last dose of lapatinib, lucitanib or AZD4547. All animal experiments were approved by the Vanderbilt Institutional Animal Care and Use Committee (IACUC protocol M/10/111).

Fluorescence in situ Hybridization (FISH)

ERBB2 gene copy number was determined by FISH using HER2 Spectrum Orange and CEP17 Spectrum Green probes (Pathvision). Enumeration of HER2 and CEP17 signals was done on 20 cells from different fields. *FGF3* gene copy number was determined by FISH using FGF3 Orange and Chromosome 11 Control Green probes (Empire Genomics). Enumeration of FGF3 and Chromosome 11 signals was done on at least 20 cells from different fields. Slides were analyzed with a reflected light fluorescent microscope (Olympus BX60) at 100×. Images of representative cells were captured using Cytovision software package (Applied Imaging).

Immunoblot analysis

BT474 cells were serum-starved overnight and treated the following day for 2 h with vehicle, 1 μM lapatinib or 1 μM AZD4547 followed by stimulation for 15 min with 50 ng/ml FGF3, FGF4, or FGF19 (R&D Systems). Cells were washed with ice-cold phosphate buffered saline (PBS) and lysed on ice in buffer containing 20 mM Tris pH 7.4, 150 mM NaCl, 1% Nonidet P-40, 1 mM EDTA plus protease and phosphatase inhibitors. Snap-frozen tumor fragments were homogenized using the TissueLyser (Qiagen) and lysed in buffer containing 50 mM Tris-HCl pH 8.0, 150 mM NaCl, 2 mM EDTA pH 8.0, 10 mM NaF, 20% glycerol, 1% Nonidet P-40 plus protease and phosphatase inhibitors. After centrifugation, protein concentration in supernatants was measured using the BCA protein assay reagent (Pierce). Proteins were separated by SDS-PAGE and transferred onto nitrocellulose membranes (Bio-Rad). Primary antibodies included: P-$HER2^{Y877}$, P-$HER2^{Y1221/2}$, P-$HER2^{Y1248}$, P-$HER3^{Y1197}$, P-$EGFR^{Y1068}$, P-Akt^{S473}, P-Akt^{T308}, Akt, P-$Erk^{T202/Y204}$, Erk, P-$FRS2\alpha^{Y436}$, P-$S6^{S240/244}$, P-$FGFR1^{Y653/4}$, P-$STAT3^{Y705}$, P-ACL^{S455}, P-BAD^{S136}, P-$PRAS40^{T246}$, and β-actin (Cell Signaling), and HER2/ERBB2 (Neomarkers). Immunoreactive bands were detected by enhanced chemiluminescence following incubation with horseradish peroxidase-conjugated secondary antibodies (Promega). Membranes were cut horizontally to probe with multiple antibodies. Blots probed with phospho-antibodies were stripped with Restore Western Blot Stripping Buffer (Thermo Fisher Scientific) and re-probed with antibodies to the total protein.

FGF4 ELISA

BT474 parental and LTR tumor lysates were analyzed using the Human FGF4 ELISA Kit (RayBiotech) according to the manufacturer's instructions.

Immunohistochemistry (IHC) and immunofluorescence

Tumor fragments were harvested and immediately fixed in 10% buffered neutral formalin for 24 h at room temperature, then dehydrated and paraffin-embedded. Five-μm sections were subjected to H&E staining and IHC using antibodies against HER2, P-HER2$^{Y1221/2}$ (Cell Signaling), Ki67 (Zymed Invitrogen) and P-FGFR$^{Y653/654}$ (Abcam**)**. Alternatively, tumor fragments were placed immediately in OCT solution and frozen on dry ice. Eight-μm frozen sections were used for IHC using an antibody against CD31 (Abcam). Trichrome staining (Sigma-Aldrich) was performed according to the manufacturer's instructions. The Histoscore for HER2 staining was graded by an expert breast pathologist (M.V.E.) using a modified scoring method previously reported by Nenutil et al. (16). Briefly, total cells and cells with positive membrane staining were counted and the percent positive cells in each high-power field (HPF) were calculated. Fields were then assigned a relative staining intensity score of 1 for low, 2 for intermediate or 3 for high staining intensity. The product of the percent positive cells and staining intensity was then derived to create a Histoscore of 0–300 for each HPF. Intra-tumor microvascular density (MVD) was scored by counting the number of endothelial cells per cluster of CD31-positive cells in 3 HPFs (17,18). Trichrome-stained tumor sections were scored in a semi-quantitative way from 0–5 based on the presence and intensity of the intra-tumor stromal collagen using a modified scoring system by Walsh et al (19). Three to five high-power fields were reviewed and an average was estimated as follows: Grade 0: Absence of collagen, Grade 1: weak staining, Grade 2: weak to moderate staining, Grade 3: moderate staining, Grade 4: moderate to strong staining, Grade 5: strong staining. Sections were scored by an expert pathologist blinded to xenograft type or treatment arm. Images were obtained using the Olympus DP2 software and an Olympus light microscope.

Indirect immunofluorescence was performed using dewaxed FFPE sections and epitopes were retrieved with citrate boiling (20). Primary antibodies against α-smooth muscle antigen (SMA), fibronectin (Sigma) and cytokeratin 8 (RDI-Fitzgerald) were incubated overnight and stained with highly cross-adsorbed goat derived secondary antibodies conjugated to AlexFluor (Life Technologies). Image acquisition was performed using a Zeiss Axioplane microscope with Metamorph (Molecular Devices) for image capture.

Lapatinib levels in xenografts

Parental BT474 and LTR xenografts treated with lapatinib and trastuzumab were harvested, weighed, homogenized, extracted and analyzed by accurate mass liquid chromatography-mass spectrometry (LC-MS) as previously described (21). A calibration curve covering the range of lapatinib concentrations observed in the tissue homogenates was prepared using a lapatinib standard for each sample set. Each sample was analyzed in triplicate.

Cell viability assay

BT474 cells were seeded in black clear-bottom 96-well plates (Greiner Bio-One) at a density of 2,000 cells per well. The next day, media was replaced with 100 μl media containing inhibitors in media containing 1% charcoal-stripped serum (CSS). After 6 days, nuclei were stained with 10 μg/ml Hoechst 33342 (Thermo Fisher Scientific) at 37°C for 20 min. Fluorescent nuclei were counted using the ImageXpress Micro XL automated microscope imager (Molecular Devices).

Statistical Analysis

The number of animals in each group was calculated to measure a 25% difference between the means of groups treated with L + T versus L + T + FGFR inhibitor with a power of 80%, a p value of 0.01, and a standard deviation of 12%, using PS Power and Sample Size Calculator software (http://biostat.mc.vanderbilt.edu/wiki/Main/PowerSampleSize). Animal experiments were conducted in a controlled and non-blinded manner. In vitro experiments were performed at least two times and at least in triplicate each time.

Unless otherwise indicated, the student's t-test was used. ANOVA and multiple comparisons tests were conducted using GraphPad Prism (GraphPad Software).

See supplementary methods for details on NGS, qRT-PCR, 3D Matrigel and apoptosis assays, gene expression analysis of the FinHER dataset, and copy number analysis of the NeoALTTO dataset.

Results

BT474 xenografts develop acquired resistance to L + T

We treated mice bearing BT474 xenografts with the combination of L + T. This treatment led to complete regression of all tumors (Fig. 1A), as reported previously (22,23). After 24 days, treatment was stopped, and mice were monitored twice weekly for tumor recurrence. Some tumors recurred as early as 9 weeks after treatment interruption. Three recurrent tumors (#32, #33, and #44) failed to respond to retreatment with L + T (Fig. 1B). These tumors were serially transplanted into treatment-naïve nude mice; treatment with L + T was resumed when tumors reached a volume ≥200 mm^3. More than 90% of tumors derived from these xenografts did not respond to L + T (Fig. S1).

LTR tumors maintain HER2 amplification, phosphorylation and HER2 downstream signaling

One possible mechanism for acquired resistance is loss of HER2 overexpression, thus abrogating HER2 dependence and the immune mechanisms of action of trastuzumab (24). Therefore, we performed HER2 FISH on FFPE sections from parental BT474 and LTR tumors. HER2 gene amplification, measured by the ratio of HER2 to chromosome 17 centromere (CEP17) probe fluorescent signals, did not differ between drug-sensitive BT474 and LTR tumors ($p = 0.61$; Fig. 1C). Accordingly, HER2 protein expression, detected by IHC, was unaltered in LTR tumors (Fig. 1D).

Next, we asked if HER2 remained activated in LTR tumors growing on continuous therapy. Treatment of parental tumors with L + T for 96 h strongly reduced levels of P-HER2 Y1221/1222 as measured by IHC (Fig. 2A). However, P-HER2 was no longer reduced in LTR tumors treated with L + T. Maintenance of P-HER2 in the majority of treated LTR tumors were seen by western blot analysis using antibodies recognizing the Y1221 autophosphorylation site and the Y877 Src site in HER2 (Fig. 2B), whereas P-EGFR^{Y1068} levels did not differ between both tumor types. Although variable, total HER2 protein levels appeared higher, on average, in LTR tumors by western blot analysis. Additionally, treatment with L + T suppressed P-Erk, P-Akt, and phosphorylation of Akt substrates [PRAS40, BAD, and ATP Citrate Lyase (ACL)] in parental tumors, but the signal was maintained in the majority of L + T-treated resistant tumors (Fig. 2B), further suggesting that treatment no longer inhibited HER2 signal transduction in drug-resistant xenografts. Finally, we performed deep sequencing of the *ERBB2* gene in LTR tumors, but did not find any mutations, arguing against acquired drug-resistant somatic alterations in HER2 (Table S1).

Lapatinib levels are reduced in LTR tumors

To determine if a decrease in drug uptake may account for the maintenance of HER2 signaling in LTR xenografts, we used accurate mass liquid chromatography-mass spectrometry (LC-MS) to measure tumor levels of lapatinib in mice treated with L + T for at least 3 days. LTR tumors contained significantly lower levels of lapatinib than drug-sensitive parental BT474 xenografts (Fig. 2C). Lapatinib has been reported to be a substrate of the ATP-binding cassette (ABC) efflux transporters, including ABCB2 (P-gp/MDR1) and ABCG2 (BCRP/MXR/ABCP) (21,25), raising the possibility that increased expression of drug efflux transporters may account for the reduced levels of lapatinib. However, expression levels of ABCB1, ABCC1, and ABCG2 mRNAs measured by quantitative RT-PCR were not altered in LTR compared to drug-sensitive tumors (Fig. S2), suggesting that the decrease in lapatinib levels in LTR tumors was not due to changes in drug efflux.

Since HER2 activation remains high in LTR tumors, we hypothesized that more complete blockade of HER2 can reverse LTR resistance. We treated cells derived from a BT474 parental xenograft and two LTR xenografts, grown in 3D Matrigel culture, with 20 μg/ml trastuzumab + increasing concentrations of lapatinib. While LTR cells maintained resistance to trastuzumab + lower concentrations of lapatinib (≤25 nM), 125 nM lapatinib + trastuzumab was able to block phoshpo-HER2 and the growth of LTR tumor-derived cells, suggesting that more complete suppression of HER2 can overcome drug resistance *in vitro* (Fig. S3).

FGFR signaling is amplified in LTR tumors

We next performed targeted capture NGS to identify somatic alterations associated with acquired resistance. Specifically, we characterized base substitutions, short insertions and deletions (indels), copy number alterations and selected fusions across 287 cancer-related genes. Of note, no mutations in *ERBB2* were found. We identified an increase in copy number of *FGF3*, *FGF4*, and *FGF19* in 1/5 LTR tumors. The *FGF3/4/19* genes reside on chromosome 11q13, along with *CCND1*. *CCND1* copy number was elevated in both LTR and BT474 parental tumors (Fig. S4). FISH, using the ratio of fluorescent signals from

probes against *FGF3* and *CEN11*, confirmed that *FGF3* copy number was increased >1.5-fold in the amplified LTR tumor relative to parental BT474 tumors (Fig. 3A). Further FISH analysis revealed that 6 additional LTR tumors (total 7/16; 43.8%) harbored *FGF3* amplification (defined by *FGF3* copy number >4 and *FGF3/CEN11* ratio >2). Likewise, FGF4 protein levels, measured by ELISA, were elevated in LTR tumors (Fig. 3B) (ELISA kits for FGF3 or FGF19 from lysates were not available). Consistent with higher levels of FGFs *in situ*, FGF-amplified LTR tumors exhibited high P-FGFR IHC staining (Fig. 3C).

In addition to exerting a tumor cell-autonomous effect in cancer cells, secreted FGF ligands can also alter the tumor microenvironment by remodeling the extracellular matrix (ECM), by paracrine activation of stromal cells such as fibroblasts, and/or by promoting angiogenesis (11). Trichrome staining of LTR tumor sections (n=8) compared to parental tumor sections (n=10) revealed marked upregulation of collagen deposition in tumor stroma (Fig. 3D–E; p=0.0008). IHC analysis of LTR tumors also revealed increased staining of smooth muscle actin (SMA) and fibronectin, markers of stromal fibroblasts. Further, a trend towards an increase in CD31+ blood vessels was observed in LTR tumors compared to parental xenografts (Fig. 3D,F; p=0.08). These microenvironmental changes are consistent with an increase in FGF pathway activation *in situ* (26).

Exogenous FGF4 induces P-ERK and promotes cell viability in the presence of HER2 inhibitors

Maintenance of P-Akt and P-Erk in LTR tumors treated with L + T led us to ask whether ligand-stimulated FGFR can activate these signaling pathways, thus bypassing targeted inhibition of HER2. Therefore, we first examined whether stimulation of BT474 cells with exogenous FGF3, FGF4 or FGF19 could activate PI3K/Akt and ERK when HER2 was blocked. BT474 cells were serum-starved overnight and then treated ± lapatinib for 2 h, followed by 15 min stimulation with FGF3, FGF4 or FGF19. Treatment with lapatinib strongly suppressed P-HER2, P-AKT and P-ERK. T308 P-AKT was modestly stimulated by FGF3 and FGF4. Of the three FGF ligands tested, only FGF4 strongly increased P-ERK and phosphorylation of the FGFR substrate, FRS2α, in the absence or presence of lapatinib (Fig. 4A), suggesting that FGF4/FGFR signaling can bypass HER2 inhibition and activate the ERK pathway. The FGFR TKI AZD4547 (15) blocked FGF4-induced P-ERK and P-FRS2α (Fig. 4B). Furthermore, exogenous FGF4 significantly attenuated the growth inhibitory effects of trastuzumab alone or L + T treatment in BT474 cells; the effects of FGF4 were reversed by the FGFR inhibitor lucitanib, a small molecule TKI with nM activity against FGFR1-3 (14) (Fig. 4C, D). Together, these data suggest that FGF4/FGFR signaling can activate the ERK pathway and partially rescue cell viability in the presence of L + T.

FGF3/4/19-amplified HER2+ cell lines are sensitive to the combination of HER2 and FGFR inhibitors

Next, we examined whether FGFR inhibition enhanced the sensitivity of HER2+/11q13-amplified HCC1954 and MDA-MB 361 human breast cancer cell lines to L + T. Treatment with L + T for 24 h led to a >2-fold increase in caspase 3/7 activity in both cell lines (Fig. S5). Lucitanib did not induce apoptosis by itself, but significantly enhanced L + T-induced

apoptosis in both cell lines, suggesting that FGFR inhibitors would synergize with HER2 inhibitors in HER2+/11q13-amplified breast cancers.

Inhibition of FGFR in vivo reverses resistance to lapatinib + trastuzumab

We next examined whether blockade of FGFR signaling with an FGFR inhibitor would restore the antitumor action of L + T against LTR tumors. For this purpose, we used lucitanib, currently in early phase clinical trials for cancers with aberrant FGFR pathway activation (11,27). We treated mice with established LTR tumors with vehicle, L + T, lucitanib alone, or the combination of L + T + lucitanib for 6 weeks. Lucitanib alone significantly inhibited tumor growth, but did not induce tumor regressions. In contrast, the 6-week treatment with L + T + lucitanib reduced tumor volume by 44% compared to that at baseline (Fig. 5A).

Treatment with lucitanib reduced P-FGFR, P-AKT and P-STAT3, but did not inhibit P-ERK as measured by immunoblot analysis of LTR tumor lysates (Fig. 5B). Likewise, IHC of LTR tumors also showed inhibition of P-FGFR by lucitanib (Fig. S6A). The FGFR inhibitor also modestly reduced levels of P-HER2^{Y877}, suggesting FGFR-induced transactivation of HER2 at the Src site in LTR tumors. Treatment with L + T did not reduce P-HER2, partially reduced P-AKT and P-ERK levels, and increased levels of P-STAT3 (Fig. 5B), a signal transducer previously shown to be involved in resistance to targeted therapies, including lapatinib (28). Treatment with lucitanib further inhibited P-AKT and prevented the induction of P-STAT3 in LTR tumors treated with L + T (Fig. 5B).

Trichrome staining of FFPE sections from LTR tumors showed that the addition of lucitanib to L + T reversed the enhanced collagen deposition seen in LTR tumors (Fig. S6B). Similarly, the addition of lucitanib strongly reduced CD31 staining and microvascular density (Supplementary Fig. S6B–C). These data suggest that the microenvironmental changes observed in the LTR tumors (Fig. 3D) are at least in part dependent on FGFR activity.

In addition to FGFR, lucitanib also inhibits the kinase activity of VEGFR1-3 (14). Therefore, to determine whether the tumor regression we observed with the combination of L + T and lucitanib was specific for FGFR, we also treated LTR tumors with a more specific inhibitor of FGFR1-3, AZD4547 (15). While AZD4547 alone did not affect tumor growth, the combination of L + T + AZD4547 significantly inhibited the growth of LTR tumors (Fig. S7A), further suggesting that FGFR inhibition can attenuate resistance to L + T. Like lucitanib, AZD4547 inhibited FGFR phosphorylation in tumor lysates (Fig. S7B), but not to the same degree as lucitanib (Fig. 5B). This result correlates in part with the lack of efficacy of single-agent AZD4547 against LTR xenografts.

Amplification of ERBB2 and FGFR pathway genes overlap in human breast cancer

Analysis of the TCGA breast cancer data revealed that nearly a quarter (23%) of *ERBB2*-amplified breast cancers also harbor amplification of *FGF3/4/19* (Fig. S8). This rate is higher than the ~15% of all breast cancers that harbor 11q13 amplification. Furthermore, *FGFR1* is amplified in 12% of the ERBB2-amplified tumors, while amplifications of *FGFR2*, *FGFR3*, and *FGFR4* are rare. These data suggest that in a significant cohort of

breast cancers, the FGFR and HER2 pathways can cooperate to promote tumor progression. Further, aberrant FGF signaling as a result of somatic alterations in the FGFR pathway may play a role in resistance to therapeutic inhibitors of HER2 in HER2 amplified breast cancers.

High FGFR1 expression correlates with a reduced benefit to adjuvant trastuzumab

Next, we asked whether amplification of FGFR pathway components correlates with resistance to HER2 inhibitors. We analyzed gene expression of *FGFR1* in HER2+ breast cancers from patients enrolled in the FinHer clinical trial, where patients were randomized after surgery to receive adjuvant chemotherapy ± trastuzumab (Fig. S9) (29). Patients with *FGFR1* expression in the bottom 80% percentile had a significantly reduced risk of disease recurrence when treated with trastuzumab (p=0.018). However, trastuzumab failed to reduce the risk of recurrence in patients with cancers in the top 20% of *FGFR1* expression (Fig. 6A).

FGFR1 and *FGF3* gene amplification associate with lower pathological complete response (pCR) to neoadjuvant anti-HER2 therapies

Finally, we interrogated whether 11q (*FGF3/4/19*) and/or *FGFR1* amplification in pre-treatment biopsies of patients enrolled in the NeoALTTO trial (3) correlated with the rate of pathological complete response (pCR) after chemotherapy plus trastuzumab, lapatinib, or L + T. Importantly, pCR rates correlate with breast cancer survival (30). A total of 134 tumors were available for copy number analysis (Fig. S10). *FGFR1* and *FGF3* amplification, particularly in ER+ tumors, correlated with a statistically lower rate of pCR (Fig. 6B). Taken together, these results suggest a causal association of alterations in the FGFR pathway with clinical resistance to anti-HER2 therapies.

Discussion

De novo and acquired resistance to HER2 inhibitors represents a major hurdle in the eradication of HER2+ breast cancer. Herein, we used HER2-dependent BT474 breast cancer xenografts to interrogate mechanisms of acquired resistance to dual HER2 blockade. Drug-resistant tumors retained HER2 gene amplification without acquired mutations in HER2 and no longer exhibited a reduction in HER2 phosphorylation upon treatment with dual anti-HER2 therapy. They also showed markedly reduced *in situ* levels of lapatinib compared to parental BT474 xenografts. We found copy number gains in *FGF3/4/19* and evidence of increased FGFR signaling in LTR tumors. Treatment with FGF4 attenuated the growth inhibitory effect of L + T *in vitro* and use of two FGFR TKIs overcame or reduced resistance to L + T *in vivo*. Finally, alterations in the FGFR pathway correlated with a worse outcome in patients with early HER2+ breast cancer treated with adjuvant and neoadjuvant anti-HER2 therapies.

Several studies have implicated FGF/FGFR signaling in attenuating the response to EGFR and HER2 inhibition. Exogenous FGF was previously shown to rescue a subset of HER2+ cell lines from lapatinib (31). The combination of lapatinib and the FGFR inhibitor dovitinib was found to reverse lapatinib resistance in SKBR3 cells in a large-scale drug combination screen (32). Dovitinib also reversed resistance to EGFR or ALK inhibitors in a subset of

patient-derived non-small cell lung cancer (NSCLC) cell lines (32). *FGFR2* amplification was found in a lapatinib-resistant HER2+ breast cancer cell line. In this same study, high FGFR2 protein levels were associated with decreased progression-free survival in a small cohort of breast cancer patients treated with lapatinib (33). Furthermore, combined inhibition of FGFR and HER2 reduced the growth of 4T1 mouse tumors more potently than either drug alone (34). In another study, combined inhibition of EGFR and FGFR reduced tumor stroma and delayed recurrence of FGFR-driven transgenic mammary tumors following FGFR inhibitor therapy (35). FGFR2 and FGFR3 have been implicated in resistance to EGFR inhibition in NSCLC (36) and trastuzumab resistance in gastric cancer (37). Further, FGFR signaling was shown to promote resistance to the KIT/PDGFR inhibitor imatinib in gastrointestinal stromal tumors through reactivation of MAPK signaling (38). These studies further support our conclusion that *FGF3/4/19* amplification can drive resistance to dual blockade of HER2 through amplification of FGFR signaling. Our study builds on these previous findings and is the first to implicate *FGF3/4/19* copy number gain in clinical resistance to HER2 inhibitors and also to report a correlation between *FGFR1* and/or *FGF3* amplification with a lesser response to HER2 inhibitors in patients with early breast cancer.

We found that stimulation of BT474 cells with FGF4 was able to induce P-FRS2 and P-ERK, whereas FGF3 and FGF19 had no effect (Fig. 4). One possibility for this difference is that FGF19 requires the β-Klotho co-receptor for signaling (39). Whether FGF4 is the primary FGF ligand that activates the FGFR pathway in *FGF3/4/19*-amplified tumors requires additional investigation. These data suggest that FGF4 may promote resistance to HER2 inhibition through bypass activation of the ERK pathway. However, we noted a discordance in that exogenous FGF4 treatment only induced partial resistance to L + T *in vitro* (Fig. 4C–D), whereas drug resistance was much more pronounced in LTR tumors *in vivo*. One possibility is that the combination of FGF3, FGF4 and FGF19 together are more effective at promoting resistance than FGF4 alone. However, neither FGF3 nor FGF19 alone at the tested concentrations were capable of inducing P-ERK. Another possibility is that increased FGF ligands may further promote resistance *in vivo* by altering the tumor microenvironment via paracrine activation of fibroblasts and endothelial cells, consistent with the altered tumor stroma we observed in LTR tumors (Fig. 3D). The combination of the FGFR TKI lucitanib with L + T was able to reverse these changes and reduce resistance (Fig. S6B–C and Fig. 5). Of note, lucitanib is currently in phase II trials in patients with breast cancer and has shown clear clinical activity against tumors harboring *FGFR1* and/or 11q13 amplifications (27).

We note that lucitanib showed single-agent activity against LTR tumors, whereas AZD4547 did not. The difference in anti-tumor activity may be due to other targets of lucitanib, such as VEGFR1-3 (14), and/or due to the more potent inhibition of P-FGFR by lucitanib *in vivo* (Figs. 5B and S7B). Whether lucitanib alone or in combination with dual HER2 blockade also inhibits growth of BT474 parental tumors is not known. Regardless, we show that combining L + T with two different FGFR inhibitors diminishes resistance in LTR tumors.

In addition to discovering *FGF3/4/19* copy number gain in a subset of LTR tumors, we also observed an increase in FGF4 protein levels and increased FGFR phosphorylation in LTR

tumors (Fig. 3B–C). Furthermore, we found that high expression and/or copy number amplification of *FGFR1* correlated with a worse outcome in patients treated with anti-HER2 therapies, suggesting that multiple ways to hyperactivate the FGFR pathway (i.e., FGF4 protein overexpression or *FGFR1* amplification/overexpression) may contribute to resistance to anti-HER2 therapy. Additional FGFR-dependent or -independent mechanisms of resistance to dual HER2 inhibition remain to be identified.

HER2 phosphorylation levels remained high in LTR tumors, suggesting that these tumors are still dependent on HER2 signaling, raising the possibility that improved inhibition of HER2 kinase activity could overcome resistance. Indeed, we found that higher doses of lapatinib + trastuzumab effectively blocked the growth of LTR tumor-derived cells *in vitro*, suggesting that more complete suppression of HER2 can overcome resistance (Fig. S3). While higher doses of lapatinib are not feasible in the clinic, more potent HER2 inhibitors, such as neratinib, may be effective in LTR tumors. Alternatively, enhancing the tumor uptake of lapatinib may also restore drug sensitivity.

While lapatinib uptake was significantly reduced in LTR tumors, we did not observe differences between levels of drug transporters *ABCB1, ABCC1*, or *ABCG2* in BT-474 parental and LTR xenografts (Fig. S2). Lapatinib is a substrate for these drug transporters. This suggests that the reduction of lapatinib in LTR vs. parental BT474 tumors is not due to altered drug transport but may be the result of FGF-induced changes in the overall tumor microenvironment. Consistent with this, LTR xenografts demonstrated marked upregulation of collagen deposition, increased staining of SMA and fibronectin, markers of stromal fibroblasts, and larger blood vessels. Changes in stromal cell proliferation and the deposition of collagen can result in changes in overall tissue heterogeneity and elasticity, as well as accompanying interstitial fluid pressure (40). Increased tissue rigidity and associated activation of integrin/focal adhesion signaling have been implicated in resistance to cancer therapies, including lapatinib (41–43). We speculate that these tumor microenvironment changes result in a reduction in lapatinib uptake in the LTR tumors as we observed.

Over 30% of HER2+ breast cancers in the TCGA harbor amplifications of *FGF3/4/19, FGFR1*, or both (Fig. S8). Therefore, our findings that FGFR pathway activation can promote resistance to HER2 inhibitors are potentially applicable to a significant cohort of patients with HER2+ breast cancer. We showed that high *FGFR1* expression correlated with de novo resistance to trastuzumab in the FinHER trial. However, we note that the number of patients in this cohort with high *FGFR1* expression is small; therefore, this correlation warrants confirmation in a larger cohort. Further, amplification of *FGFR1* and *FGF3* correlated with lower pCR rates following neoadjuvant anti-HER2 therapy in the NeoALTTO trial. We note that this correlation was only significant in ER+ patients (Fig. 6B). While this could be due to the relatively small size of the clinical cohort, this result is not inconsistent with our findings in ER+/HER2+ BT474 xenografts. In addition, amplification of both *FGFR1* and 11q13, where the *FGF3/4/19* genes reside, are more prevalent in ER+ tumors and associated with endocrine resistance (13,44,45). These studies suggest that aberrant activation of the FGFR pathway is associated with primary/intrinsic resistance to therapeutic inhibition of HER2. Future studies should examine whether FGF/FGFR signaling is also altered in tumors that have *acquired* resistance to HER2 inhibitors.

On this basis, we propose that the combination of HER2 and FGFR inhibitors should be prospectively investigated in patients with HER2+ breast cancer harboring somatic alterations in the FGFR pathway.

Supplementary Material

Refer to Web version on PubMed Central for supplementary material.

Acknowledgments

We thank Teresa Dugger and Violeta Sánchez for expert technical assistance and Luigi Formisano and Brent Rexer for helpful discussions.

Financial Support: This work was supported by American Cancer Society 118813-PF-10-070-01-TBG (JTG) and Department of Defense BC093376 (JTG) Postdoctoral Fellowship Awards; Department of Defense Postdoctoral Fellowship Award BC103785 (ABH); NIH/NCI K12 Award CA090625 (ABH); NCI R01 grant CA080195 (CLA); NIH Breast Cancer Specialized Program of Research Excellence (SPORE) grant P50 CA98131; and Vanderbilt-Ingram Cancer Center Support Grant P30 CA68485.

References

1. Slamon DJ, Clark GM, Wong SG, Levin WJ, Ullrich A, McGuire WL. Human breast cancer: correlation of relapse and survival with amplification of the HER-2/neu oncogene. Science. 1987; 235(4785):177–82. [PubMed: 3798106]
2. Arteaga CL, Engelman JA. ERBB receptors: from oncogene discovery to basic science to mechanism-based cancer therapeutics. Cancer Cell. 2014; 25(3):282–303. DOI: 10.1016/j.ccr.2014.02.025 [PubMed: 24651011]
3. Baselga J, Bradbury I, Eidtmann H, Di Cosimo S, de Azambuja E, Aura C, et al. Lapatinib with trastuzumab for HER2-positive early breast cancer (NeoALTTO): a randomised, open-label, multicentre, phase 3 trial. Lancet. 2012; 379(9816):633–40. DOI: 10.1016/S0140-6736(11)61847-3 [PubMed: 22257673]
4. Swain SM, Kim SB, Cortes J, Ro J, Semiglazov V, Campone M, et al. Pertuzumab, trastuzumab, and docetaxel for HER2-positive metastatic breast cancer (CLEOPATRA study): overall survival results from a randomised, double-blind, placebo-controlled, phase 3 study. Lancet Oncol. 2013; 14(6): 461–71. DOI: 10.1016/S1470-2045(13)70130-X [PubMed: 23602601]
5. Gianni L, Pienkowski T, Im YH, Roman L, Tseng LM, Liu MC, et al. Efficacy and safety of neoadjuvant pertuzumab and trastuzumab in women with locally advanced, inflammatory, or early HER2-positive breast cancer (NeoSphere): a randomised multicentre, open-label, phase 2 trial. Lancet Oncol. 2012; 13(1):25–32. DOI: 10.1016/S1470-2045(11)70336-9 [PubMed: 22153890]
6. Hanker AB, Pfefferle AD, Balko JM, Kuba MG, Young CD, Sanchez V, et al. Mutant PIK3CA accelerates HER2-driven transgenic mammary tumors and induces resistance to combinations of anti-HER2 therapies. Proc Natl Acad Sci U S A. 2013; 110(35):14372–7. DOI: 10.1073/pnas.1303204110 [PubMed: 23940356]
7. Rexer BN, Chanthaphaychith S, Dahlman K, Arteaga CL. Direct inhibition of PI3K in combination with dual HER2 inhibitors is required for optimal antitumor activity in HER2+ breast cancer cells. Breast Cancer Res. 2014; 16(1):R9.doi: 10.1186/bcr3601 [PubMed: 24451154]
8. Loibl S, von Minckwitz G, Schneeweiss A, Paepke S, Lehmann A, Rezai M, et al. PIK3CA mutations are associated with lower rates of pathologic complete response to anti-human epidermal growth factor receptor 2 (her2) therapy in primary HER2-overexpressing breast cancer. J Clin Oncol. 2014; 32(29):3212–20. DOI: 10.1200/JCO.2014.55.7876 [PubMed: 25199759]
9. Koboldt DC, Fulton RS, McLellan MD, Schmidt H, Kalicki-Veizer J, McMichael JF, et al. Comprehensive molecular portraits of human breast tumours. Nature. 2012; 490(7418):61–70. DOI: 10.1038/nature11412 [PubMed: 23000897]

10. Cerami E, Gao J, Dogrusoz U, Gross BE, Sumer SO, Aksoy BA, et al. The cBio cancer genomics portal: an open platform for exploring multidimensional cancer genomics data. Cancer discovery. 2012; 2(5):401–4. DOI: 10.1158/2159-8290.CD-12-0095 [PubMed: 22588877]
11. Dieci MV, Arnedos M, Andre F, Soria JC. Fibroblast growth factor receptor inhibitors as a cancer treatment: from a biologic rationale to medical perspectives. Cancer discovery. 2013; 3(3):264–79. DOI: 10.1158/2159-8290.CD-12-0362 [PubMed: 23418312]
12. Elbauomy Elsheikh S, Green AR, Lambros MB, Turner NC, Grainge MJ, Powe D, et al. FGFR1 amplification in breast carcinomas: a chromogenic in situ hybridisation analysis. Breast Cancer Res. 2007; 9(2):R23.doi: 10.1186/bcr1665 [PubMed: 17397528]
13. Turner N, Pearson A, Sharpe R, Lambros M, Geyer F, Lopez-Garcia MA, et al. FGFR1 amplification drives endocrine therapy resistance and is a therapeutic target in breast cancer. Cancer Res. 2010; 70(5):2085–94. DOI: 10.1158/0008-5472.CAN-09-3746 [PubMed: 20179196]
14. Bello E, Colella G, Scarlato V, Oliva P, Berndt A, Valbusa G, et al. E-3810 is a potent dual inhibitor of VEGFR and FGFR that exerts antitumor activity in multiple preclinical models. Cancer Res. 2011; 71(4):1396–405. DOI: 10.1158/0008-5472.CAN-10-2700 [PubMed: 21212416]
15. Gavine PR, Mooney L, Kilgour E, Thomas AP, Al-Kadhimi K, Beck S, et al. AZD4547: an orally bioavailable, potent, and selective inhibitor of the fibroblast growth factor receptor tyrosine kinase family. Cancer Res. 2012; 72(8):2045–56. DOI: 10.1158/0008-5472.CAN-11-3034 [PubMed: 22369928]
16. Nenutil R, Smardova J, Pavlova S, Hanzelkova Z, Muller P, Fabian P, et al. Discriminating functional and non-functional p53 in human tumours by p53 and MDM2 immunohistochemistry. J Pathol. 2005; 207(3):251–9. DOI: 10.1002/path.1838 [PubMed: 16161005]
17. Wang D, Stockard CR, Harkins L, Lott P, Salih C, Yuan K, et al. Immunohistochemistry in the evaluation of neovascularization in tumor xenografts. Biotechnic & histochemistry : official publication of the Biological Stain Commission. 2008; 83(3–4):179–89. DOI: 10.1080/10520290802451085 [PubMed: 18846440]
18. Weidner N. Current pathologic methods for measuring intratumoral microvessel density within breast carcinoma and other solid tumors. Breast Cancer Res Treat. 1995; 36(2):169–80. [PubMed: 8534865]
19. Walsh AJ, Cook RS, Lee JH, Arteaga CL, Skala MC. Collagen density and alignment in responsive and resistant trastuzumab-treated breast cancer xenografts. Journal of biomedical optics. 2015; 20(2):26004.doi: 10.1117/1.JBO.20.2.026004 [PubMed: 25700233]
20. Owens P, Pickup MW, Novitskiy SV, Giltnane JM, Gorska AE, Hopkins CR, et al. Inhibition of BMP signaling suppresses metastasis in mammary cancer. Oncogene. 2014; doi: 10.1038/onc.2014.189
21. Polli JW, Humphreys JE, Harmon KA, Castellino S, O'Mara MJ, Olson KL, et al. The role of efflux and uptake transporters in [N-{3-chloro-4-[(3-fluorobenzyl)oxy]phenyl}-6-[5-(<2-(methylsulfonyl)ethyl]amino }methyl)-2-furyl]-4-quinazolinamine (GW572016, lapatinib) disposition and drug interactions. Drug Metab Dispos. 2008; 36(4):695–701. doi dmd.107.018374 [pii] 10.1124/dmd.107.018374 [doi]. [PubMed: 18216274]
22. Garrett JT, Sutton CR, Kuba MG, Cook RS, Arteaga CL. Dual blockade of HER2 in HER2-overexpressing tumor cells does not completely eliminate HER3 function. Clin Cancer Res. 2013; 19(3):610–9. DOI: 10.1158/1078-0432.CCR-12-2024 [PubMed: 23224399]
23. Garrett JT, Sutton CR, Kurupi R, Bialucha CU, Ettenberg SA, Collins SD, et al. Combination of antibody that inhibits ligand-independent HER3 dimerization and a p110alpha inhibitor potently blocks PI3K signaling and growth of HER2+ breast cancers. Cancer Res. 2013; 73(19):6013–23. DOI: 10.1158/0008-5472.CAN-13-1191 [PubMed: 23918797]
24. Mittendorf EA, Wu Y, Scaltriti M, Meric-Bernstam F, Hunt KK, Dawood S, et al. Loss of HER2 amplification following trastuzumab-based neoadjuvant systemic therapy and survival outcomes. Clin Cancer Res. 2009; 15(23):7381–8. DOI: 10.1158/1078-0432.CCR-09-1735 [PubMed: 19920100]
25. Polli JW, Olson KL, Chism JP, John-Williams LS, Yeager RL, Woodard SM, et al. An unexpected synergist role of P-glycoprotein and breast cancer resistance protein on the central nervous system penetration of the tyrosine kinase inhibitor lapatinib (N-{3-chloro-4-[(3-fluorobenzyl)oxy]phenyl}-6-[5-(<2-(methylsulfonyl)ethyl]amino }methyl)-2-furyl]-4-

quinazolinamine; GW572016). Drug Metab Dispos. 2009; 37(2):439–42. doi dmd.108.024646 [pii] 10.1124/dmd.108.024646 [doi]. [PubMed: 19056914]

26. Turner N, Grose R. Fibroblast growth factor signalling: from development to cancer. Nat Rev Cancer. 2010; 10(2):116–29. DOI: 10.1038/nrc2780 [PubMed: 20094046]
27. Soria JC, DeBraud F, Bahleda R, Adamo B, Andre F, Dientsmann R, et al. Phase I/IIa study evaluating the safety, efficacy, pharmacokinetics, and pharmacodynamics of lucitanib in advanced solid tumors. Ann Oncol. 2014; 25(11):2244–51. DOI: 10.1093/annonc/mdu390 [PubMed: 25193991]
28. Lee HJ, Zhuang G, Cao Y, Du P, Kim HJ, Settleman J. Drug resistance via feedback activation of Stat3 in oncogene-addicted cancer cells. Cancer Cell. 2014; 26(2):207–21. DOI: 10.1016/j.ccr.2014.05.019 [PubMed: 25065853]
29. Joensuu H, Kellokumpu-Lehtinen PL, Bono P, Alanko T, Kataja V, Asola R, et al. Adjuvant docetaxel or vinorelbine with or without trastuzumab for breast cancer. N Engl J Med. 2006; 354(8):809–20. DOI: 10.1056/NEJMoa053028 [PubMed: 16495393]
30. Cortazar P, Zhang L, Untch M, Mehta K, Costantino JP, Wolmark N, et al. Pathological complete response and long-term clinical benefit in breast cancer: the CTNeoBC pooled analysis. Lancet. 2014; 384(9938):164–72. DOI: 10.1016/S0140-6736(13)62422-8 [PubMed: 24529560]
31. Wilson TR, Fridlyand J, Yan Y, Penuel E, Burton L, Chan E, et al. Widespread potential for growth-factor-driven resistance to anticancer kinase inhibitors. Nature. 2012; 487(7408):505–9. DOI: 10.1038/nature11249 [PubMed: 22763448]
32. Crystal AS, Shaw AT, Sequist LV, Friboulet L, Niederst MJ, Lockerman EL, et al. Patient-derived models of acquired resistance can identify effective drug combinations for cancer. Science. 2014; 346(6216):1480–6. DOI: 10.1126/science.1254721 [PubMed: 25394791]
33. Azuma K, Tsurutani J, Sakai K, Kaneda H, Fujisaka Y, Takeda M, et al. Switching addictions between HER2 and FGFR2 in HER2-positive breast tumor cells: FGFR2 as a potential target for salvage after lapatinib failure. Biochem Biophys Res Commun. 2011; 407(1):219–24. DOI: 10.1016/j.bbrc.2011.03.002 [PubMed: 21377448]
34. Issa A, Gill JW, Heideman MR, Sahin O, Wiemann S, Dey JH, et al. Combinatorial targeting of FGF and ErbB receptors blocks growth and metastatic spread of breast cancer models. Breast Cancer Res. 2013; 15(1):R8.doi: 10.1186/bcr3379 [PubMed: 23343422]
35. Holdman XB, Welte T, Rajapakshe K, Pond A, Coarfa C, Mo Q, et al. Upregulation of EGFR signaling is correlated with tumor stroma remodeling and tumor recurrence in FGFR1-driven breast cancer. Breast Cancer Res. 2015; 17:141.doi: 10.1186/s13058-015-0649-1 [PubMed: 26581390]
36. Ware KE, Marshall ME, Heasley LR, Marek L, Hinz TK, Hercule P, et al. Rapidly acquired resistance to EGFR tyrosine kinase inhibitors in NSCLC cell lines through de-repression of FGFR2 and FGFR3 expression. PLoS One. 2010; 5(11):e14117.doi: 10.1371/journal.pone.0014117 [PubMed: 21152424]
37. Piro G, Carbone C, Cataldo I, Di Nicolantonio F, Giacopuzzi S, Aprile G, et al. An FGFR3 Autocrine Loop Sustains Acquired Resistance to Trastuzumab in Gastric Cancer Patients. Clin Cancer Res. 2016; 22(24):6164–75. DOI: 10.1158/1078-0432.CCR-16-0178 [PubMed: 27267856]
38. Li F, Huynh H, Li X, Ruddy DA, Wang Y, Ong R, et al. FGFR-Mediated Reactivation of MAPK Signaling Attenuates Antitumor Effects of Imatinib in Gastrointestinal Stromal Tumors. Cancer discovery. 2015; 5(4):438–51. DOI: 10.1158/2159-8290.CD-14-0763 [PubMed: 25673643]
39. Kurosu H, Choi M, Ogawa Y, Dickson AS, Goetz R, Eliseenkova AV, et al. Tissue-specific expression of betaKlotho and fibroblast growth factor (FGF) receptor isoforms determines metabolic activity of FGF19 and FGF21. J Biol Chem. 2007; 282(37):26687–95. DOI: 10.1074/jbc.M704165200 [PubMed: 17623664]
40. Lu P, Weaver VM, Werb Z. The extracellular matrix: a dynamic niche in cancer progression. J Cell Biol. 2012; 196(4):395–406. DOI: 10.1083/jcb.201102147 [PubMed: 22351925]
41. Egeblad M, Rasch MG, Weaver VM. Dynamic interplay between the collagen scaffold and tumor evolution. Curr Opin Cell Biol. 2010; 22(5):697–706. DOI: 10.1016/j.ceb.2010.08.015 [PubMed: 20822891]

42. Lin C, Pelissier FA, Zhang H, Lakins J, Weaver VM, Park C, et al. Microenvironment rigidity modulates responses to the HER2 receptor tyrosine kinase inhibitor lapatinib via YAP and TAZ transcription factors. Mol Biol Cell. 2015; doi: 10.1091/mbc.E15-07-0456

43. Hirata E, Girotti MR, Viros A, Hooper S, Spencer-Dene B, Matsuda M, et al. Intravital imaging reveals how BRAF inhibition generates drug-tolerant microenvironments with high integrin beta1/FAK signaling. Cancer Cell. 2015; 27(4):574–88. DOI: 10.1016/j.ccell.2015.03.008 [PubMed: 25873177]

44. Elsheikh S, Green AR, Aleskandarany MA, Grainge M, Paish CE, Lambros MB, et al. CCND1 amplification and cyclin D1 expression in breast cancer and their relation with proteomic subgroups and patient outcome. Breast Cancer Res Treat. 2008; 109(2):325–35. DOI: 10.1007/s10549-007-9659-8 [PubMed: 17653856]

45. Roy PG, Pratt N, Purdie CA, Baker L, Ashfield A, Quinlan P, et al. High CCND1 amplification identifies a group of poor prognosis women with estrogen receptor positive breast cancer. Int J Cancer. 2010; 127(2):355–60. DOI: 10.1002/ijc.25034 [PubMed: 19904758]

Statement of Translational Relevance

Dual blockade of HER2, with the combinations of trastuzumab and lapatinib or trastuzumab and pertuzumab, has been shown to be superior to trastuzumab alone. However, acquired resistance to anti-HER2 therapies remains a problem. We found an increase in *FGF3/4/19* gene copy number in HER2-overexpressing xenografts with acquired resistance to lapatinib + trastuzumab. This was accompanied by an increase in FGFR phosphorylation, reduced levels of lapatinib in drug-resistant tumors, and changes in the tumor microenvironment. Combining FGFR inhibitors with lapatinib + trastuzumab led to regression of the drug-resistant tumors. Finally, high *FGFR1* gene expression and amplification of *FGFR1* and *FGF3* correlated with an inferior clinical response to anti-HER2 therapies in patients with early HER2+ breast cancer. These findings support profiling genes in the FGFR pathway in tumors with acquired resistance to HER2-directed therapies and the clinical investigation of FGFR and HER2 inhibitors in these treatment-refractory HER2+ breast cancers.

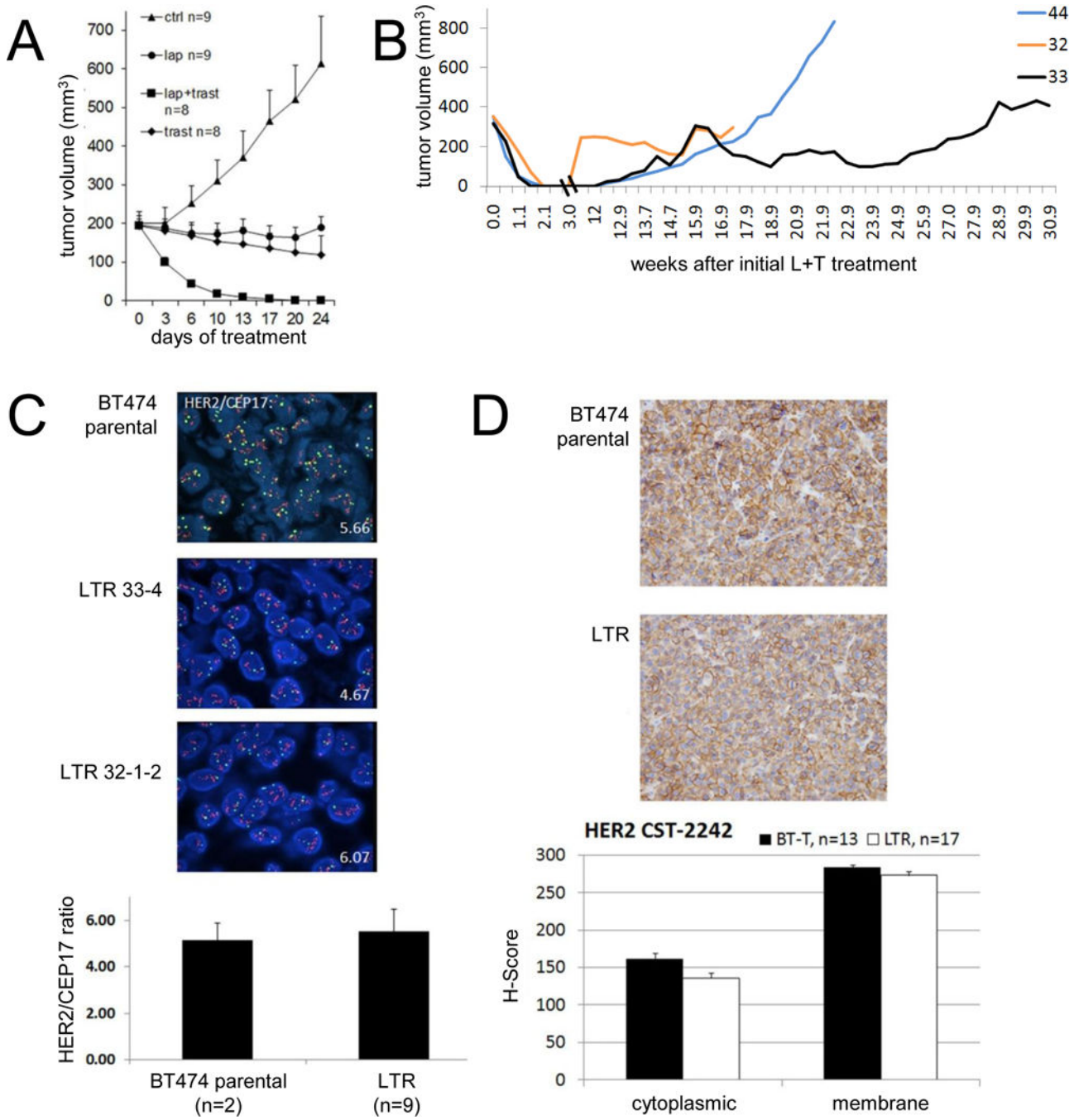

Figure 1. HER2 gene amplification is maintained in LTR tumors

(**A**) Athymic female mice were injected with BT474 cells and treated with vehicle, 100 mg/kg of lapatinib by oral gavage daily, 20 mg/kg of trastuzumab given intraperitoneally twice weekly or the combination (lap + trast). Treatment was administered for 24 days. Each data point represents the mean tumor volume ± SEM (n=8–9). (**B**). L + T-treated mice from (A) were monitored for tumor recurrence twice weekly. Once recurrent tumors reached a volume ≥200 mm^3, L + T were resumed and continued until the time of tumor harvest. (**C**) *ERBB2* gene copy number was determined by FISH. p=0.61, student's t-test. (**D**). IHC

analysis of HER2 in tumor sections. Shown at top are representative images. Bottom panel: Quantitative comparison of cytoplasmic and membrane HER2 histoscore.

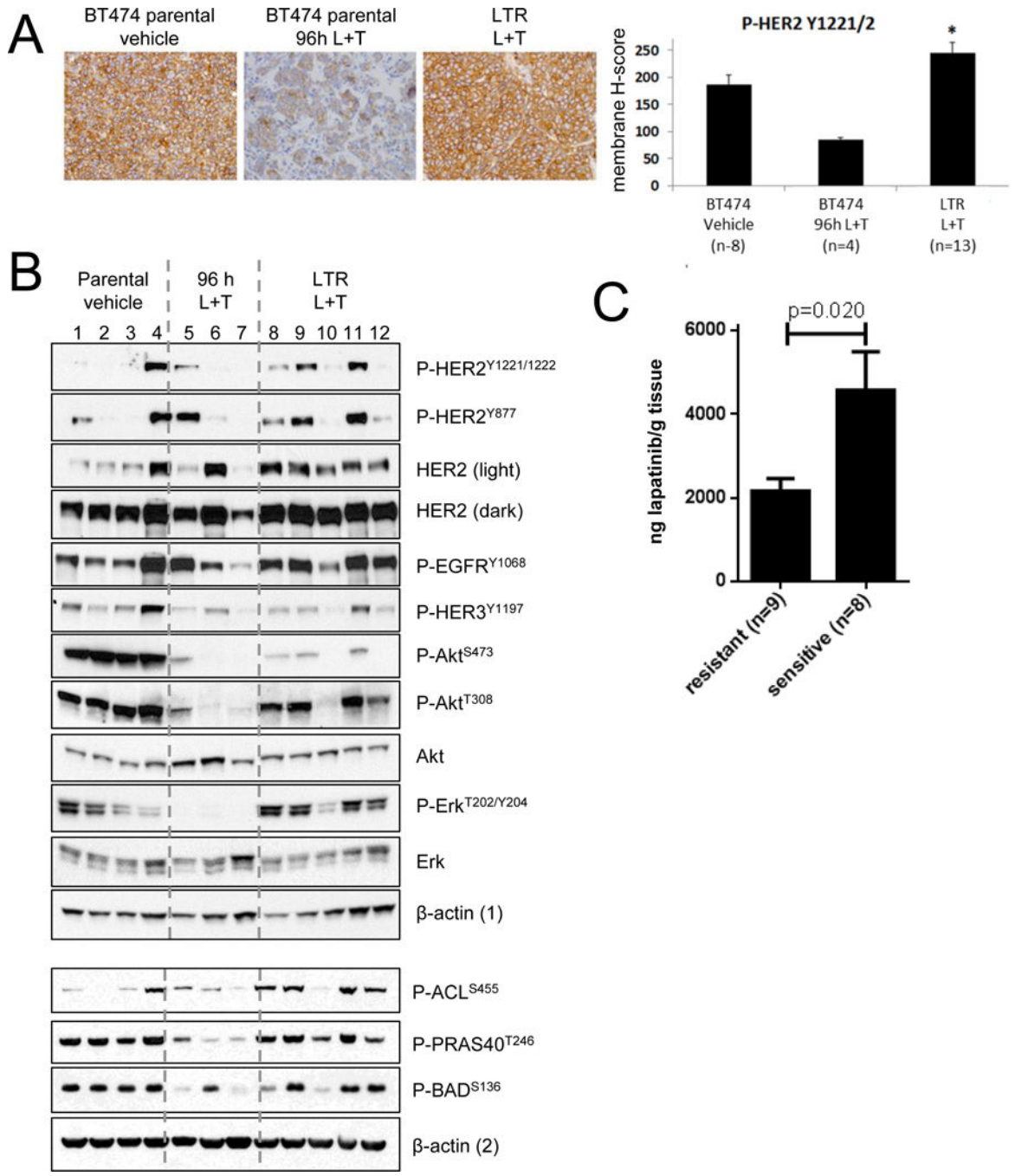

Figure 2. LTR xenografts maintain phosphorylated HER2 and post-receptor signaling

(**A**) IHC analysis of P-Y1221/2 P-HER2 in tumor sections. Groups of mice bearing parental BT474 xenografts received vehicle or L + T for 96 h only (96 h L + T) whereas those bearing LTR tumors were treated continuously; both groups of mice were sacrificed 24 h after the last treatment with trastuzumab and 1 h after the last dose of lapatinib. Shown at top are representative images. Bottom panel: Quantitative comparison of membrane P-HER2 histoscore. *p<0.05 compared to parental BT474 untreated tumors. (**B**) Tumors were treated as described in (A). Tumor lysates were subjected to immunoblot analysis with the indicated

antibodies. The same lysates were run on 2 separate gels (the horizontal black line indicates separate gels). (**C**) Mice bearing drug-sensitive and -resistant (LTR) tumors were treated for 72 h or longer with lapatinib and sacrificed 1 h after the last lapatinib dose. Tumors were harvested and tissue sections were weighed, homogenized, extracted and analyzed by accurate mass LC-MS. Each sample was analyzed in triplicate. Concentrations are reported in ng lapatinib/gram of tissue.

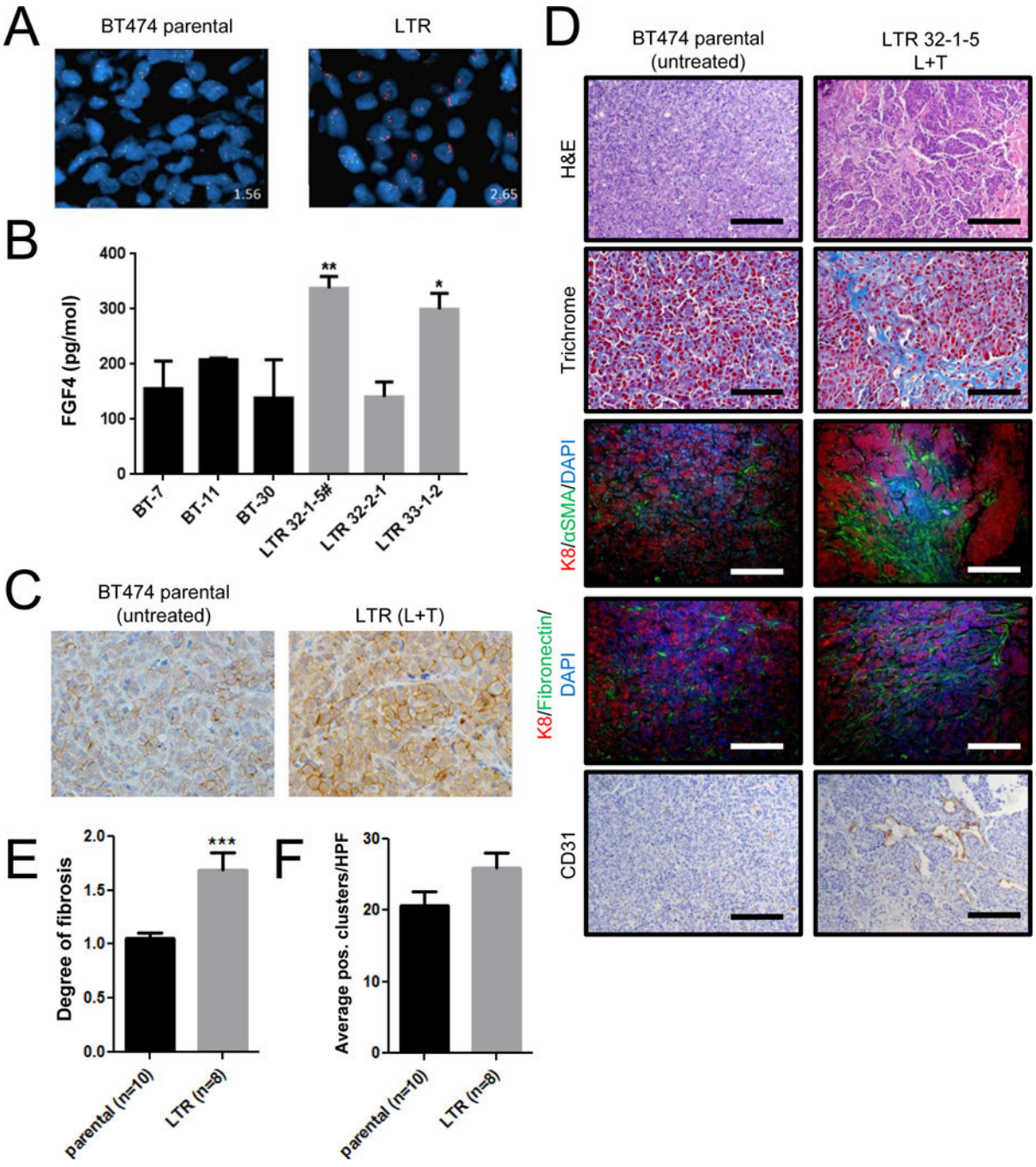

Figure 3. LTR xenografts amplify FGF ligands and downstream signaling

(**A**) *FGF3* gene copy number in parental and LTR tumors was determined by FISH. (**B**) Lysates from tumors treated with vehicle (BT) or L + T (LTR) were subjected to ELISA for FGF4. (*p<0.05, **p<0.01, relative to BT-T parental tumors, 1-way ANOVA with Tukey's multiple comparison test). Data represent the average ± SD of duplicate reactions. (**C**) IHC analysis of P-FGFR$^{Y653/654}$ in tumor sections. (**D**) FFPE sections from parental BT474 (n=10) and LTR (n=8)_ xenografts were stained or subjected to IHC with the indicated antibodies. Scale bar = 200 μm. **(E)** Trichrome staining was quantified as described in

Materials & Methods. Each bar represents the average ± SEM (***p<0.001, student's t-test). (**F**) CD31 staining was quantified as described in Materials & Methods. Each bar represents the average ± SEM (p=0.08, student's t-test).

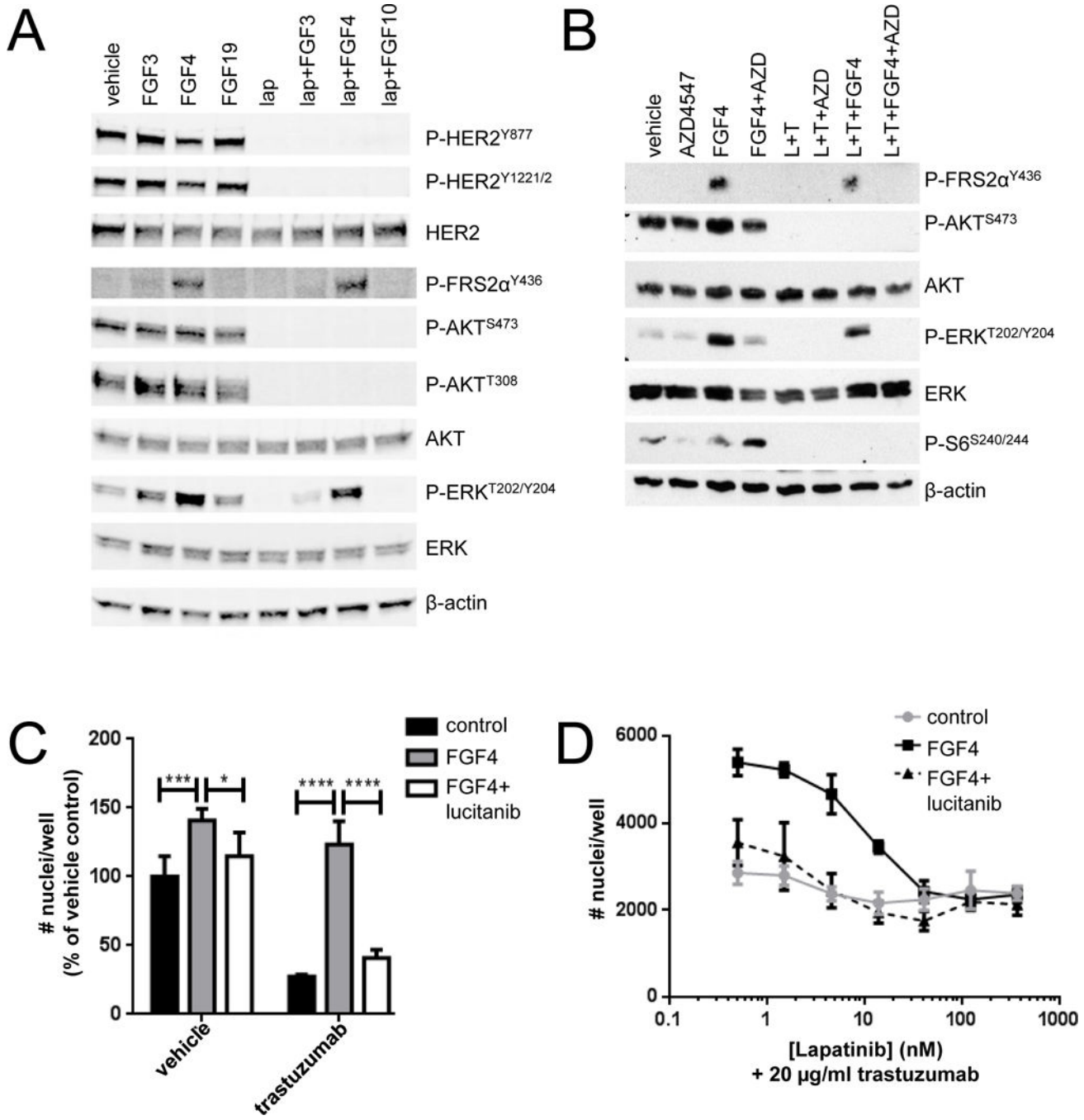

Figure 4. Exogenous FGF4 activates ERK and promotes resistance to HER2 inhibition

(**A**) Parental BT474 cells grown *in vitro* were serum-starved overnight and treated the following day for 2 h with vehicle or 1 μM lapatinib followed by stimulation for 15 min with 50 ng/ml FGF3, FGF4, or FGF19. Whole cell lysates were subjected to immunoblot analysis with the indicated antibodies. **(B)** BT474 cells were serum-starved overnight and treated the following day for 2 h with vehicle, 20 μg/ml trastuzumab + 1 μM lapatinib, or 1 μM AZD4547, and then stimulated for 15 min with 50 ng/ml FGF4. Whole cell lysates were subjected to immunoblot analysis with the indicated antibodies. **(C)** BT474 cells growing in

low serum (1% CSS) were treated with vehicle or 50 ng/ml FGF4 ± 2 μM lucitanib and ± 20 μg/ml trastuzumab. After 6 days, nuclei were stained with Hoechst and scored using the ImageXpress system. Data represent the average ± SD of 4 replicate wells (*p<0.05; ***p<0.001; ****p<0.0001, 2-way ANOVA followed by Bonferroni's multiple comparisons test). **(D)** BT474 cells growing in 1% CSS were treated with increasing concentrations of lapatinib (0.5–300 nM) + 20 μg/ml trastuzumab ± 50 ng/ml FGF4 ± 2 μM lucitanib for 6 days. Hoechst-stained nuclei were scored using the ImageXpress system. Data represent the average ± SD of 4 replicate wells.

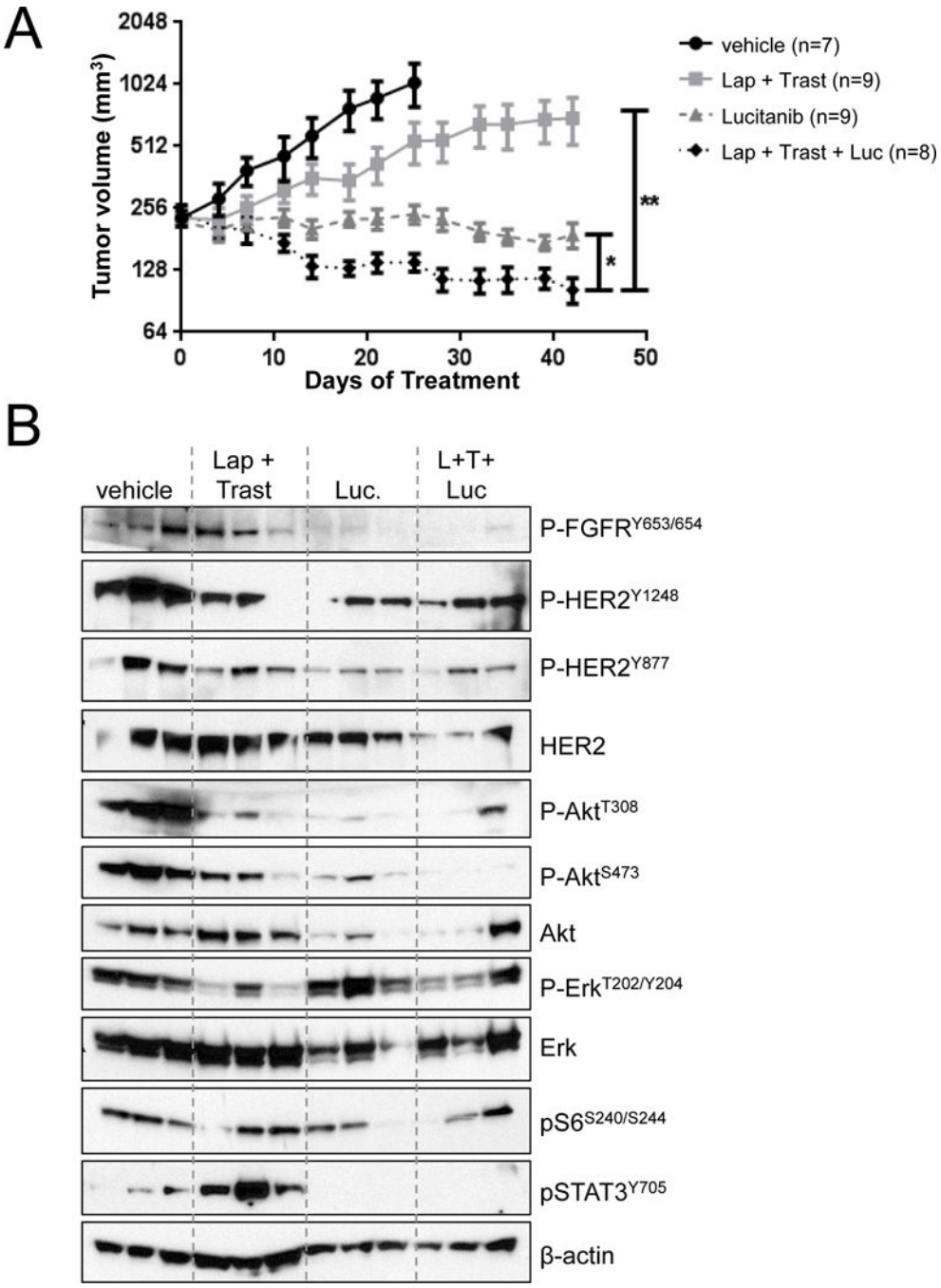

Figure 5. FGFR inhibition abrogates resistance to lapatinib + trastuzumab

(**A**) Mice bearing LTR tumors measuring ≥200 mm^3 were treated with 1) vehicle, 2) L + T, 3) lucitanib, or 4) L + T + lucitanib for 6 weeks. Each data point represents the mean tumor volume ± SEM. The Y axis is shown on a Log2 scale (*p<0.05; **p<0.01, Student's t-test). **(B)** Tumors were harvested at the completion of treatment (6 weeks). Whole tumor lysates were prepared as indicated in Materials & Methods and subjected to immunoblot analysis with the indicated antibodies.

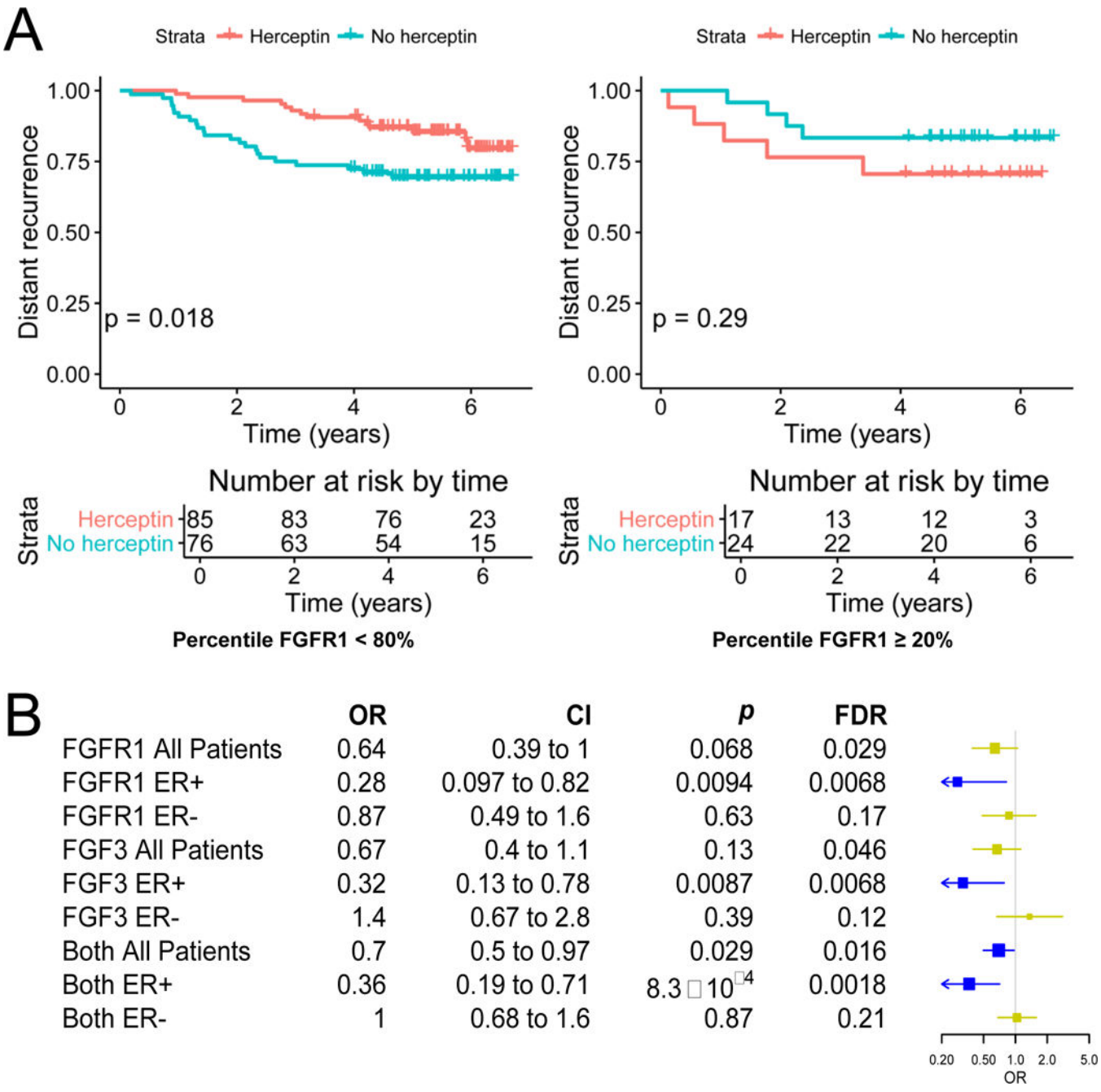

Figure 6. Alterations in *FGFR1* and/or *FGF3* correlate with a lower clinical response to anti-HER2 therapies

(**A**) *FGFR1* mRNA expression was measured by gene expression microarrays in RNA extracted from FFPE tumor sections (n = 202) collected pre-treatment as part of the FinHer trial. Kaplan-Meier curves according to *FGFR1* expression were generated by dichotomizing patients at the top expression level quintile (≥20%) or bottom 80%). **(B)** The copy number status of *FGFR1* and *FGF3* was assessed in pre-treatment biopsies from 134 HER2+ breast cancers from patients treated with neoadjuvant chemotherapy + trastuzumab, lapatinib, or the combination in the NeoALTTO trial. Logistic regression of the pCR in *FGFR1*- or

FGF3-amplified patients is shown. Both, *FGF3*+*FGFR1* amplified; OR, odds ratio; CI, confidence interval; FDR, false discovery rate.